JOURNAL OF GUIDANCE, CONTROL, AND DYNAMICS
Vol. 34, No. 2, March–April 2011

Engineering Notes

Costate Approximation and Comparisons Between Improved and Classical Indirect Trajectory Optimization

Roger L. Barron*
Stanardsville, Virginia 22973

DOI: 10.2514/1.51515

Introduction

INDIRECT methods of two-point boundary-value (TPBV) trajectory optimization, guidance, and control are generally built upon a calculus-of-variations foundation [1,2] using specified performance indices written in the form of definite integrals of continuous functions having continuous first and second derivatives between initial and final times. Predictive shooting of trajectories is the tool most widely used to initialize the costate differential equations associated with indirectly optimized TPBV solutions. In the interest of fast, reliable initialization convergence, one seeks improvements that provide 1) reductions of costate system differential order, search-space dimensionality, and multiple-costate interactions; 2) reductions of final-state sensitivities to small maladjustments of initial costates and unanticipated en route state changes; and 3) analytic propagation of costates between time boundaries.

References [3,4] introduced trim-referenced performance indices and approximations of costate differential equations (CDEs) with time-linear algebraic functions used to reduce the computational workload for costate initialization. Time-linear costates, taken alone, do not generally satisfy the first-variation necessary conditions required for high-order and nonlinear vehicle dynamics. But incorporation of suitable trim-reference functions in performance index (PI) specifications has the effect of compensating for vehicle dynamics without placing the burden for such compensation on the costate system. Thus, approximate time-linear costates and trim referencing can lead jointly to near-replication of classical optimum trajectories along with the benefit of a less arduous costate initialization search.

A refinement would be to use a family of time-series polynomials representing costate systems with greater fidelity than can be obtained using only time-linear functions. This could be important for high-order vehicle dynamics, with or without PI trim references. For an Nth-order physical system, one could begin by approximating the costate system with a family of N polynomials for which the polynomial of highest degree involves time raised to the Nth power. For a second-order physical system, one of the two costates would thus be approximated by a first-degree polynomial and the other costate would be approximated by a second-degree polynomial. Adding a third order, the third costate would be approximated by a polynomial of third degree, and so forth. Such families of approximated costate functions would be, of course, time-integrable. The complete family would involve time-series polynomials comprising a total of N undetermined parameters, these being the initial values of the costates. (For any indirect TPBV method involving an Nth-order physical system, N initial costates must be determined.)

The primary questions prompting this Engineering Note are as follows:

1) If approximate CDEs are inexact, what claim can be made for optimality?

2) Is it legitimate to modify the performance index and compare results with a classical method for which the index is not so modified?

In addressing these questions, this Note first examines use of trim-referenced performance indices considered alone, then in combination with basic time-linear CDEs. A pair of elementary applications is studied. Performance results with the improved method are compared with results for the classical indirect synthesis method, and it is shown that results for the two methods are nearly identical. Challenging future applications may require the higher-degree costate representations just mentioned.

The method of costate approximations per se does not modify the performance index or reduce CDE order. However, use of trim-reference functions in a modified PI can reduce requirements on the costate approximations, as clearly evidenced by Example 1 in the next section. The approximated costate family is reduced to degree $N-1$, lower than required absent trim referencing in the PI. The lower-degree costate family works in concert with a new plant excitation function that stems from the trim-referenced PI and produces essentially the same plant response as obtained via the full classical procedure. Thus an external observer probably could not discern whether the solution had been developed via the improved or classical indirect method.

Because the costate approximations are lower-degree representations of classical CDEs, they are generally less sensitive to disturbances and initialization errors than the exact functions.

This Note emphasizes trajectory performance comparisons. Costate initializations were obtained manually for all Example 2 cases. In doing so, it was observed qualitatively that search convergence was achieved more easily using the improved procedure. Quantitative analysis of convergence properties using candidate numerical initialization algorithms is a subject for future study.

Example 1: TPBV Control of Linear Time-Invariant Plant

For Example 1, consider a linear time-invariant plant characterized by the scalar differential equation:

$$\ddot{x} + a_1\dot{x} + a_0 x = bu \tag{1}$$

In steady-state operation ($\ddot{x} = 0$), the trim excitation level is

$$u_{\text{trm}} = (a_1\dot{x} + a_0 x)/b \tag{2}$$

Table 1 summarizes the optimum control laws derived for this plant when applying the improved and classical indirect methods.

A simple comparison of the improved and classical methods via simulation is for the case of fixed t_f. Suppose the boundary conditions at $t_0 = 0$ are $x_0 = \dot{x}_0 = 0$ and the boundary conditions at $t_f = 1$ are $x_f = 1$ and $\dot{x}_f = 0$. Take $u_0 = 0$ and $a_0 = a_1 = b = 1$. From theory,† the expected response for the new method is a sigmoidal curve for $x(t)$, obtained with $\lambda_{1_0} = 12$, $\lambda_{1_f} = -12$, and $\lambda_2 = 24$. Using a modified Nelder–Mead search [5], the costate initial values returned by the search using the new method were

Received 7 July 2010; revision received 25 October 2010; accepted for publication 14 November 2010.

*Independent Consultant, 7593 Celt Road. Senior Member AIAA.

†The analytical solution for exact initialization of the approximated costates in Example 1 is $\lambda_{1_0} = 4(-\Delta\dot{x} + 3\Delta x/\tau_f)/(b^2K\tau_f)$, $\lambda_2 = 12(\Delta\dot{x} + 2\Delta x/\tau_f)/(b^2K\tau_f^2)$, $\Delta x \equiv x_f - x_0 - \dot{x}_0\tau_f$, $\Delta\dot{x} \equiv \dot{x}_f - \dot{x}_0$, and $\tau_f \equiv t_f - t_0$.

Table 1 Comparison for Example 1 of indirect optimization methods

Method	PI integrand[a]	Excitation function	First CDE	Second CDE
Improved	$(u-u_{trm})^2+\lambda_1 f_1+\lambda_2 f_2$	$u=b\lambda_1/2+(a_1V+a_0x)/b$	$\dot{\lambda}_1=-\lambda_2$	$\dot{\lambda}_2=0$ ($\lambda_2=$ constant)
Classical	$u^2+\lambda_1 f_1+\lambda_2 f_2$	$u=b\lambda_1/2$	$\dot{\lambda}_1=a_1\lambda_1-\lambda_2$	$\dot{\lambda}_2=a_0\lambda_1$

[a] Differential constraints are $f_1=\dot{V}+a_1V+a_0x-bu$ and $f_2=\dot{x}-V$.

$\lambda_{1_0}=12.1084$ and $\lambda_{2_c}=24.3252$, which produced the dashed curves for $x(t)$, $V(t)$, $\lambda_1(t)$, and λ_2 shown in Figs. 1–4, respectively. In the figures, solid curves pertain to the improved formulation, dashed curves to the classical.

For the classical method, the same predictive search algorithm returned $\lambda_{1_0}=11.7341$, and $\lambda_{2_0}=21.3369$.

It is seen that the trim-referenced PI provided an enhanced excitation function that fully compensated the plant dynamics (a_1 and a_0 terms) and led to a simplified but successful CDE family.

Example 2: Guidance of Collinear Tail-Chase Intercept and Rendezvous

Although in the previous example the trim-reference function provided full compensation of plant dynamics, removing such responsibility from the costate system, there may be reason to employ an actuation reference that is less complete in its compensation. Example 2 illustrates such a case; the actuation reference pertains to deviations from minimum thrust required to maintain static equilibrium in straight and level flight. Again, basic time-linear costate approximations are successful in nearly duplicating classical performance.

In Example 2, optimum trajectories are sought for collinear tail-chase, variable-t_f, variable-thrust rendezvous maneuvers when both the guided vehicle and a target object move horizontally along collinear trajectories at the same altitude. The path of the target is assumed to be known. This example might apply to guidance of an air vehicle as it approaches a tanker aircraft to be refueled, throttle control to reach a specified trajectory waypoint in minimum time with specified final velocity, or intercept (with high final closing velocity) of another air vehicle. In some applications the final time may be fixed in advance, but in most instances (as herein) t_f is variable and subject to optimization.

A PI similar to that of Example 1 is defined:

$$J \equiv \int_{t_0}^{t_f} [K_0 + (\Delta T)^2/K]\,\mathrm{d}t \tag{3}$$

wherein the added constant Lagrange multiplier K_0 introduces an isoperimetric condition that pertains to minimization of $t_f - t_0$, and

$$\Delta T = T - T_{\mathrm{mss}} \tag{4}$$

where T is thrust and T_{mss} is the minimum steady-state thrust required for static trim in level flight. It is assumed that $T+\Delta T$ is continuously variable between fixed limits. Lags in thrust response are ignored. The thrust increment relates to displacements from the ideal operating condition.

For unaccelerated (trimmed) straight and level flight[‡]: $T_{\mathrm{mss}}=2mg\sqrt{a/c}$, $\alpha_{\mathrm{mss}}=\sqrt{a/c}$, and $V^2_{\mathrm{mss}}=(2mg/\rho Sc)\sqrt{c/a}$, where m is vehicle mass, g is gravity acceleration, a and c are axial and normal aerodynamic body-axes force coefficients, S is a reference area, and ρ is local air density. It is assumed that all of these parameters are constants, α_{mss} is small, and wind gusts and ballistic wind are absent.

Equations of Motion (Example 2)

To maintain level flight of the guided vehicle, it is necessary that the aerodynamic angle of attack be maintained at $\alpha=2mg/(\rho V^2 Sc)$. Ignoring winds and using x to denote position on the horizontal axis of the tail-chase maneuver,

$$m\ddot{x} = (T-A)\cos\alpha - N\sin\alpha = T\cos\alpha - \rho V^2 S(a\cos\alpha + c\sin^2\alpha)/2 \tag{5}$$

where A and N are the guided-vehicle axial and normal forces, respectively.

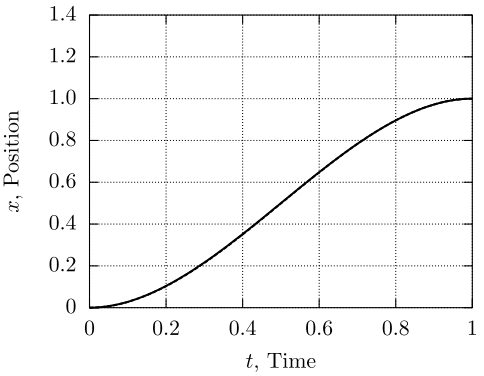

Fig. 1 Example 1 position responses for improved and classical methods.

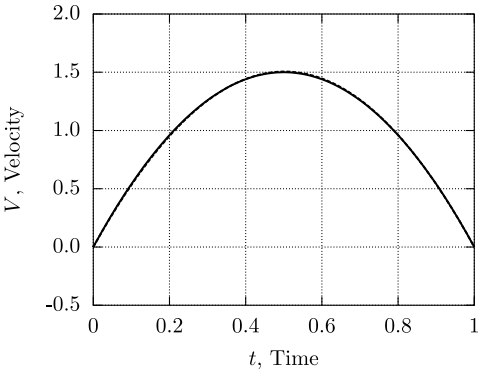

Fig. 2 Example 1 velocity responses for improved and classical methods.

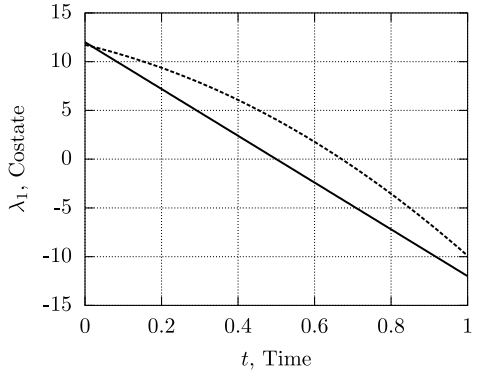

Fig. 3 Example 1 costate 1 vs t for improved and classical methods.

[‡]For climb angle γ, $\alpha_{\mathrm{mss}}=(mg\cos\gamma)/(\frac{1}{2}\rho V^2_{\mathrm{mss}}Sc+mg\sin\gamma)$, $T_{\mathrm{mss}}=\frac{1}{2}\rho V^2_{\mathrm{mss}}Sa+mg(\sin\gamma+\alpha_{\mathrm{mss}}\cos\gamma)$, and $V^2_{\mathrm{mss}}=(2mg/\rho Sc)(\sqrt{(c/a)}\cos\gamma-\sin\gamma)$.

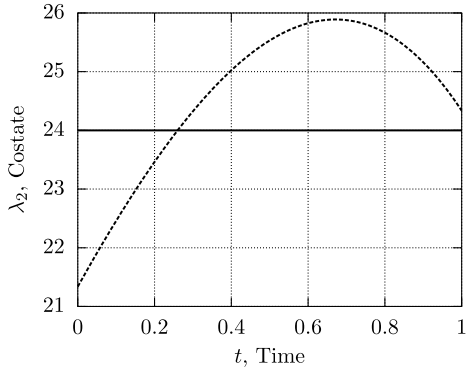

Fig. 4 Example 1 costate 2 vs t for improved and classical methods.

Approximating for small α, one obtains

$$m\ddot{x} = T - \rho V^2 Sa/2 - 2(mg)^2/\rho V^2 Sc \tag{6}$$

Introducing the notation $V = \dot{x}$, the equation of motion becomes

$$\dot{V} = (T - C_1 V^2 - C_2/V^2)/m \tag{7}$$

where $C_1 = \rho Sa/2 = \text{const}$, $C_2 = 2(mg)^2/(\rho Sc) = \text{const}$, and C_1V^2 and C_2/V^2 are the form-plus-parasite and induced air-resistance forces, respectively.

Constrained Performance Index (Example 2)

Incorporating the equations of motion within a constrained PI,

$$F \equiv K_0 + (T - T_{\text{mss}})^2/K + \lambda_1[\dot{V} - (T - C_1V^2 - C_2/V^2)/m] + \lambda_2(\dot{x} - V) \tag{8}$$

where K is a constant (nominally unity) available for scaling purposes.

The following command function, CDEs, and variable-t_f transversality conditions are obtained:

$$T = K\lambda_{1_f}/(2m) + T_{\text{mss}} \tag{9}$$

$$\dot{\lambda}_1 = 2\lambda_1(C_1V - C_2/V^3)/m - \lambda_2 \tag{10}$$

$$\dot{\lambda}_2 = 0 \qquad (\lambda_2 = \text{const}) \tag{11}$$

$$\lambda_{1_f}\delta V_f + \lambda_2 \delta x_f = 0 \quad (\text{where } \delta V_f = \delta x_f = 0) \tag{12}$$

$$K_0 + (T_f - T_{\text{mss}})^2/K - \lambda_{1_f}(\dot{V}_f - \dot{V}_{T_f}) - \lambda_2(V_f - V_{T_f}) = 0 \tag{13}$$

Note that the CDEs, Eqs. (10) and (11), require constant $\dot{\lambda}_2$, but not constant $\dot{\lambda}_1$.

In Eq. (13), substituting Eqs. (9) and (10) at $t = t_f$,

$$K_0 + \left(\frac{K}{2m}\lambda_{1_f}\right)^2 \Big/ K - \lambda_{1_f}\left[\left(T_{\text{mss}} + \frac{K}{2m}\lambda_{1_f} - C_1V_f^2 - C_2/V_f^2\right)\Big/ m - \dot{V}_T\right] - \lambda_2(V_f - V_{T_f}) = 0 \tag{14}$$

(Particularly if $K_0 \neq 0$, a careful selection between the two roots of this λ_{1_f} quadratic is required.) V_f should be the desired final total velocity of the guided vehicle. There is no mathematical difference between rendezvous solutions and variable-t_f intercepts if V_f is specified.

For the classical method applied to Example 2 for variable-t_f maneuver optimization,

$$T = K\lambda_1/(2m) \tag{15}$$

and T_{mss} disappears in Eq. (14).

Costate Approximation with New Method (Example 2)

With the plant dynamics of Eq. (1) for Example 1, specification of the $(u - u_{\text{trm}})^2$ integrand penalty led to $\dot{\lambda}_1 = \text{const}$ and $\lambda_2 = \text{const}$. However, in Example 2, provisional specification of a $(T - T_{\text{mss}})^2$ integrand penalty in the PI produces the CDE of Eq. (10), where $\dot{\lambda}_1$ is generally not constant, even though λ_2 is constant. The improved-method simulations for Example 2 replace Eq. (10) with the simple approximation $\dot{\lambda}_1 = \dot{\lambda}_{1_c} = \text{const}$. This evokes a question put forth in the Introduction: Is one justified in treating $\dot{\lambda}_1$ as constant? Simulation results provide an affirmative answer.

The following summary of algorithms simulated in Example 2 uses (a)mss to denote the primary improved algorithm using forward costate propagation, (b)mss to denote an equivalent algorithm using backward costate propagation, (c) to denote the classical algorithm used for comparison with the proposed algorithm, and (c)mss to denote a pseudoclassical procedure in which the PI is referenced to T_{mss}. Note that (a) and (b) are regarded as three-parameter algorithms because they return τ_f, λ_{1_0}, and λ_2. Internally, (a) and (b) compute $\dot{\lambda}_1(t)$ via formula and search only on two parameters, τ_f and λ_2.

Prior specification of K_0 and K in the PI was required, of course. Inputs to the algorithms were the guided-vehicle parameters m, a, c, and S; the geophysical data ρ and g; and the target trajectory estimates x_{T_0}, V_{T_0}, and $\dot{V}_T$ (all assumed to be constant). The future path of the target was computed via Taylor series: $x_T(\tau_f) = x_{T_0} + \tau_f(V_{T_0} + \tau_f\dot{V}_T/2)$ and $V_T(\tau_f) = V_{T_0} + \tau_f\dot{V}_T$, assuming constant $\dot{V}_T$.

$\dot{\lambda}_{1_0}$ *Forward Analytical Propagation: Algorithm* (a)mss

1) For given trial values of τ_f and λ_2, compute λ_{1_f} via the quadratic solution.

2) Compute $\lambda_{1_0} = \lambda_{1_f} - \tau_f\dot{\lambda}_{1_0}$, noting that $\dot{\lambda}_{1_0} = 2\lambda_{1_0}(C_1V_0 - C_2/V_0^3)/m - \lambda_2$, so

$$\lambda_{1_0} = (\lambda_{1_f} + \tau_f\lambda_2)/[1 + 2\tau_f(C_1V_0 - C_2/V_0^3)/m] \tag{16}$$

3) Shoot a trial trajectory using numerical integration (starting at x_0, V_0) employing the optimum thrust command function, Eq. (15), and $\lambda_1(t) = \lambda_{1_0} + (t - t_0)\dot{\lambda}_{1_0}$.

4) For $t = t_f$ on the trial trajectory, combine the position and velocity errors in a score function,

$$\text{Score} = W_0(x_{T_f} - \hat{x}_f)^2 + W_1(V_{T_f} - \hat{V}_f)^2 \tag{17}$$

where the W's are non-negative constants and $\hat{()}$ denotes a predicted value.

5) Generate next set of τ_f and λ_2 trial values and repeat until convergence is obtained.

$\dot{\lambda}_{1_f}$ *Reverse Analytical Propagation: Algorithm* (b)mss

In the above algorithm (a), change the second step to read as follows: Compute $\lambda_{1_0} = \lambda_{1_f} - \tau_f\dot{\lambda}_{1_f}$, noting that $\dot{\lambda}_{1_f} = 2\lambda_{1_f}(C_1V_f - C_2V_f^3)/m - \lambda_2$, so

$$\lambda_{1_0} = \lambda_{1_f}[1 - 2\tau_f(C_1V_f - C_2/V_f^3)/m] + \tau_f\lambda_2 \tag{18}$$

Algorithms (c) *and* (c)mss

Algorithms (c) and (c)mss, that is, the classical and pseudo-classical algorithms, respectively, (the latter using a trim-referenced PI), both employ time-varying costate rates and a three-parameter initialization search $(\tau_f, \lambda_{1_0}, \lambda_2)$, whereas (a)mss and (b)mss search only τ_f and λ_2.

With (c) and (c)mss, using given trial values of τ_f, λ_{1_0}, and λ_2, the system of equations (including the vehicle equations of motion) is integrated forward, using stepwise-numerical procedures, to obtain predicted final position and velocity errors. Additionally, the simultaneous numerical integration of the exact CDE for $\dot{\lambda}_1(t)$ provides $\hat{\lambda}_{1_f}$, whereby the Eq. (14) transversality condition (quadratic solution) determines the final-time costate error, $\lambda_{1_f} - \hat{\lambda}_{1_f}$, where λ_{1_f} is provided by Eq. (14). If the final costate error is acceptably small, a composite performance measure for the given trial may be computed as in Eq. (17), adding a term $W_3(\lambda_{1_f} - \hat{\lambda}_{1_f})^2$.

A legitimate trajectory shot for any of the above algorithms is one that satisfies the relevant first-variation necessary conditions and does not violate inequality constraints on T, V, and α.

Simulation Results (Example 2)

The variable-t_f rendezvous guidance algorithms described in the previous section were tested in computer simulations employing the parameters and parameter values listed below in Table 2. A notional small turbojet aircraft (perhaps an unmanned aerial vehicle) weighing 2500 kgf (5511 lb) was envisioned. For minimum steady-state (mss) thrust required during straight and level flight of this aircraft, $\alpha_{\text{mss}} = 0.09128$ rad (5.230 deg), $T_{\text{mss}} = 4476$ N (1006 lb), and $V_{\text{mss}} = 71.5$ m/s (234 ft/s).

The variable-t_f solutions required close attention to the Eq. (14) transversality condition on λ_{1_f}. With the improved method, an analytical solution for λ_{1_0} was used with reverse integration[§] via Eq. (18). The effect was to eliminate λ_{1_0} from the initialization search. The remaining τ_f and λ_2 search was found to be dramatically easier than the τ_f, λ_{1_0}, and λ_2 search required by the classical method.

Terminal accuracies of the four methods were comparable and depended, of course, on the levels specified for acceptable final position and velocity errors. The stop rule used in the initialization searches was $-7 \text{ cm} < x_{T_f} - x_f < 0$ and $-6 \text{ cm/s} < V_{T_f} - V_f < 0$. The negative bias in these thresholds was intentional so that the guided vehicle would have a small residual closing velocity at the time of rendezvous.

The maneuver duration, $\tau_f = t_f - t_0$, was responsive to the value of K_0. Considering the new and classical performance index integrands, one has for the new method $K_0 + (T - T_{\text{mss}})^2/K$, and for the classical method $K_0' + T^2/K$, denoting K_0 for equivalent classical solutions by K_0'. For equivalence, $K_0 + (T - T_{\text{mss}})^2/K = K_0' + T^2/K$. Therefore, $K_0' = K_0 - T_{\text{mss}}(2T - T_{\text{mss}})/K$. Typically, $T \approx 2T_{\text{mss}}$ in the present experiments, so $K_0' \approx K_0 - 3T_{\text{mss}}^2/K$. Thus if $K = 5000$, then $T_{\text{mss}} = 4476$ and $K_0 = 2034$, and one has $K_0' \approx -10,000$ for equivalence. As determined by simulation, the transversality condition required $K_0' = -9305$.

Relative levels of fuel consumption were calculated as proportional to the total thrust impulse applied over the (t_0, t_f) interval, assuming a constant thrust-specific fuel consumption (TSFC) rate throughout the admissible thrust range ($T_{\min} \leq T \leq T_{\max}$). There was no significant difference in fuel consumption among the four algorithms tested. Other cost measures were also computed, as noted below.

The comparisons showed no discernible differences in trajectory shape and smoothness between the improved and classical methods.

Comparisons of computational burden considered analytical vs stepwise-numerical costate propagation; differential order of costate system and consequent dimensionality of initialization search space; behavior of the partial derivatives of final physical states to small changes in τ_f, λ_{1_0}, and λ_2; and number of search trials needed to satisfy terminal accuracy requirements. Computational burden, qualitatively assessed during manual searches, was substantially reduced by use of the improved methods.

[§]Either $\dot{\lambda}_{1_0}$ or $\dot{\lambda}_{1_f}$ may be selected, with λ_{1_0} computed via Eq. (16) or Eq. (18), respectively.

Table 2 Simulation parameters (Example 2)

Parameter	Value assigned	Units
m	2500	kgm
a	0.025	unitless
c	3.0	rad^{-1}
S	35	m^2
ρ	1.0	kgm/m^3
g	9.80665	m/s^2
$T_{\max}$	20	kN
$T_{\min}$	1.5	kN
K_0	(See text)	unitless
K	5000	N^2
W_0	1	m^{-2}
W_1	100	(m/s)^2
W_3	(Not used)	(kgm/N)$^{-2}$
τ_f	(See text)	s
λ_1	(See text)	kgm/N
λ_2	(See text)	N^2/s
x_0	0	m
V_0	71.5	m/s
$\dot{V}_0$	0	m/s^2
x_{T_0}	1000	m
V_{T_0}	78.65	m/s
$\dot{V}_T$	0.66	m/s^2

Table 3 summarizes numerical results for the Example 2 simulations. Note that trajectory cost factors are tabulated four ways: τ_f and total integrals of $(\Delta T)^2$, T^2, and T. As K_0 and K_0' were adjusted to more positive settings, maneuver duration was shortened (in absence of thrust saturation). Table 3 makes clear that the trajectory behavior of the several algorithms being compared was virtually identical. (As mentioned above, K_0 and K_0' were selected for equivalence between performance indices.)

In summary, the improved methods produced the same trajectories as the classical methods. It would be manifestly better to use the improved methods because of their reduced computational burden and reduced sensitivities to initialization errors and state-observation errors.

Figure 5 is a graph of acceleration responses; it also demonstrates the validity of the small-α assumption made in Example 2.

Figure 6 shows a representative collinear rendezvous maneuver using $K_0 = 2500$ in algorithm (a)mss or, equally, (b)mss.

Figures 7–9 show that the rendezvous maneuver of Fig. 6 is essentially identical for algorithms (a)mss, (c)mss, and (c), provided that K_0 was adjusted to the values 2500, 5865, and -4783, respectively, as shown in Table 3. For these comparisons, the solid curves correspond to (a)mss, the dashed curves correspond to (c)mss, and the dotted curves correspond to (c). Figure 7 presents the guided-vehicle position histories, Fig. 8 presents the velocity histories, and Fig. 9 presents the thrust histories.

As in Example 1, the costate histories in Example 2 are not identical, as seen in Fig. 10. Referring to Table 2, one sees that all three algorithms have comparable maneuver penalties, as judged via integrals of $(\Delta T)^2$, T^2, and T.

Potentially, an optimum path-to-go could be computed periodically for $t_0 \leq t < t_f$, given $x(t)$ and the specified $x(t_f)$. When it is operationally necessary for guidance commands to be adaptive to internal model deficiencies, vehicle malfunctions or damage, external disturbances, end-state changes, and/or own-vehicle navigation errors, path-to-go updates should be used. Such updates would also benefit performance of approximated costate functions because the approximation accuracies generally improve as the prediction horizon shrinks. En route updates were not used in the present study.

Discussion

For purposes of illustration, consider a fourth-order linear time-invariant plant for which

Table 3 Rendezvous simulation results

Algorithm	τ_f	$\int_{t_0}^{t_f}[\,]\,dt$ $10^{-8}(\Delta T)^2$	$10^{-8}T^2$	$10^{-4}T$	Remarks
(*a*)mss and (*b*)mss	56.59	13.91	46.00	49.63	Improved methods, $K_0 = 0$
(*c*)mss	56.59	13.81	46.95	49.69	Pseudoclassical method, $K_0 = 2034$
(*c*)	56.59	13.83	46.93	49.63	Classical method, $K_0' = -9305$
(*a*)mss and (*b*)mss	50.40	15.14	44.82	44.44	Improved methods, $K_0 = 2500$
(*c*)mss	50.40	14.99	44.71	44.49	Pseudoclassical method, $K_0 = 5865$
(*c*)	50.40	15.00	44.70	44.45	Classical method, $K_0' = -4783$

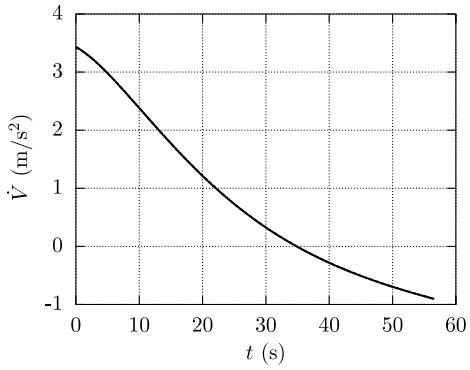

Fig. 5 $\dot{V}$ for (*a*)mss algorithm during rendezvous maneuver. (Curves for small-α and large-α assumptions are indistinguishable.)

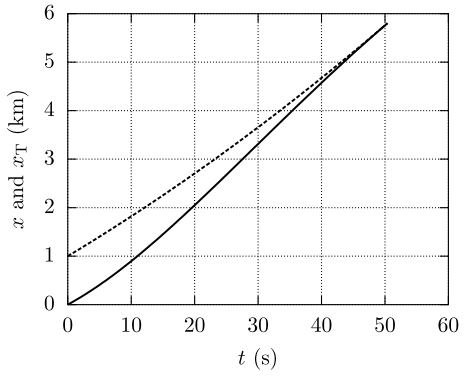

Fig. 6 Rendezvous using (*a*)mss algorithm with $K_0 = 2500$. Rendezvous occurs at 50.40 s. The dashed curve is the target position, and solid curve is the guided-vehicle position.

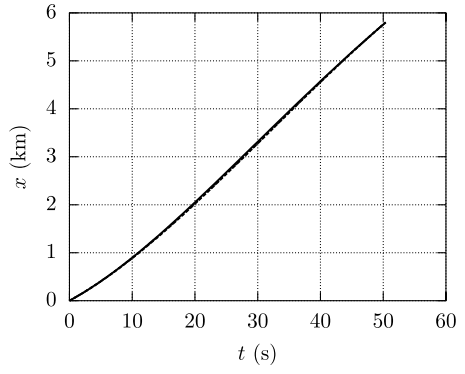

Fig. 7 Positions of guided vehicle vs time during rendezvous maneuvers at $t_f = 50.40$ s. Solutions are obtained with three algorithms. (Curves are indistinguishable.)

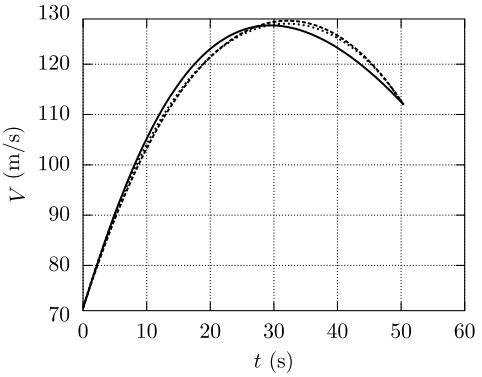

Fig. 8 Velocities of guided vehicle vs time during rendezvous maneuvers corresponding to Fig. 7.

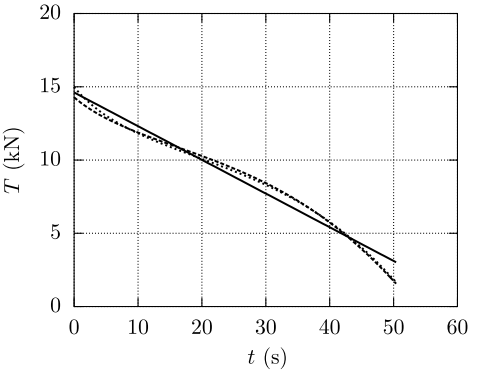

Fig. 9 Thrust histories for rendezvous maneuvers with three algorithms. $t_f = 50.40$ s.

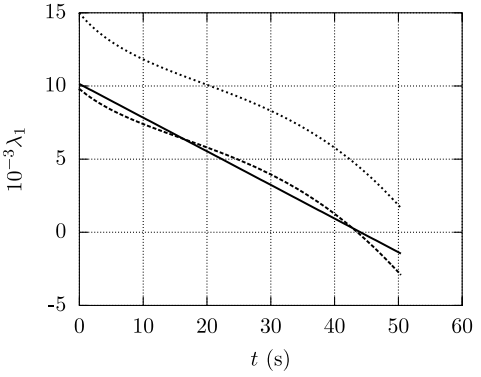

Fig. 10 Costate λ_1 history for rendezvous maneuvers with three algorithms. $t_f = 50.40$ s.

$$a_4 \frac{\mathrm{d}^4 x}{\mathrm{d}t^4} + \cdots + a_1 \dot{x} + a_0 x = bu \tag{19}$$

and the control performance index is written as

$$J = \int_{t_0}^{t_f} [u^2 + \lambda_1(\dot{x} - v) + \lambda_2(\dot{v} - w) + \lambda_3(\dot{w} - z) + \lambda_4(a_4 \dot{z} + a_3 z + a_2 w + a_1 v + a_0 x - bu)] \mathrm{d}t \tag{20}$$

In previous sections of this Note, costates are numbered in the opposite sequence.

The Euler–Lagrange first-variation necessary conditions yield the excitation function

$$u = (b/2)\lambda_4 \tag{21}$$

and the costate differential equations:

$$\dot{\lambda}_1 = a_0 \lambda_4, \qquad \dot{\lambda}_2 = a_1 \lambda_4 - \lambda_1$$
$$\dot{\lambda}_3 = a_2 \lambda_4 - \lambda_2, \qquad \dot{\lambda}_4 = a_3 \lambda_4 - \lambda_3 \tag{22}$$

Defining $\tau = t - t_0$, let $\dot{\lambda}_1(\tau)$ be approximated by the constant $a_0 \lambda_{4_0}$. Then,

$$\lambda_1(\tau) = \lambda_{1_0} + a_0 \lambda_{4_0} \tau \tag{23}$$

$$\lambda_2(\tau) = \lambda_{2_0} + (a_1 \lambda_{4_0} - \lambda_{1_0})\tau - \tfrac{1}{2} a_0 \lambda_{4_0} \tau^2 \tag{24}$$

$$\lambda_3(\tau) = \lambda_{3_0} + (a_2 \lambda_{4_0} - \lambda_{2_0})\tau - \tfrac{1}{2}(a_1 \lambda_{4_0} - \lambda_{1_0})\tau^2 + \tfrac{1}{6} a_0 \lambda_{4_0} \tau^3 \tag{25}$$

$$\lambda_4(\tau) = \lambda_{4_0} + (a_3 \lambda_{4_0} - \lambda_{3_0})\tau - \tfrac{1}{2}(a_2 \lambda_{4_0} - \lambda_{2_0})\tau^2 + \tfrac{1}{6}(a_1 \lambda_{4_0} - \lambda_{1_0})\tau^3 - \tfrac{1}{24} a_0 \lambda_{4_0} \tau^4 \alpha \tag{26}$$

An alternative approximation family could proceed from the assumption that $\dot{\lambda}_1(\tau) = \lambda_{1_0} e^{c\tau}$, where c is a constant obtained by fitting exact $\dot{\lambda}$ CDE data from a selection of representative classically optimum trajectories.

The evidence from Examples 1 and 2 in this Note indicates that when using trim-referenced performance indices, the polynomial costate approximations can be further simplified by a reduction of one degree, to wit, for plants of second order:

$$\lambda_1(\tau) = \lambda_{1_0} \tag{27}$$

$$\lambda_2(\tau) = \lambda_{2_0} - \lambda_{1_0} \tau \tag{28}$$

Extension to (and beyond)

$$\lambda_3(\tau) = \lambda_{3_0} - \lambda_{2_0} \tau + \tfrac{1}{2} \lambda_{1_0} \tau^2 \tag{29}$$

$$\lambda_4(\tau) = \lambda_{4_0} - \lambda_{3_0} \tau + \tfrac{1}{2} \lambda_{2_0} \tau^2 - \tfrac{1}{6} \lambda_{1_0} \tau^3 \tag{30}$$

should be verified in future work.

Conclusions

The performance of an improved indirect method for trajectory optimization, a method that uses trim-referenced performance indices jointly with time-linear algebraic functions (the simplest time-series polynomial approximation) to approximate costate behavior, has been compared with the performance of classical indirect methods for two illustrative applications. System state responses for the improved method are found in close agreement with their corresponding classical trajectory solutions, with the comparison being predicated upon terminal accuracy, maneuver duration, fuel consumption, and trajectory shape and smoothness. The improved method has the potential to reduce the computational burden of costate initialization because of reduced differential order of the costate system, lower dimensionality of the initialization search space, reduced sensitivities of final-state values to small errors in initial costates, analytical propagation of costates. It has also been demonstrated that a single unique costate system is not a requisite for near optimality of trajectories in the classical sense, and it is suggested that a family of nonlinear time-series polynomials could be used to approximate costate behavior for more complex systems.

Acknowledgments

Cleon M. Chick III performed the simulations in this study. Andrew R. Barron of Yale University and Ping Lu of Iowa State University provided helpful critiques and suggestions, as did the reviewers.

References

[1] Kirk, D. E., *Optimal Control Theory: An Introduction*, Prentice–Hall, Englewood Cliffs, NJ, 1970, Chap. 2, pp. 29–46.

[2] Ben-Asher, J. Z., *Optimal Control Theory with Aerospace Applications*, AIAA, Reston, VA, 2010, Chaps. 3 and 4.

[3] Barron, R. L., and Chick, C. M., III, "Improved Indirect Method for Air-Vehicle Trajectory Optimization," *Journal of Guidance, Control, and Dynamics*, Vol. 29, No. 3, May–June 2006, pp. 643–652. doi:10.2514/1.16228

[4] Barron, R. L., and Chick, C. M., III, "Trim-Reference Functions for Indirect Method of Trajectory Optimization," *Journal of Guidance, Control, and Dynamics*, Vol. 30, No. 4, July–Aug. 2007, pp. 1189–1193. doi:10.2514/1.28725

[5] Press, W. H., Teukolsky, S. A., Vetterling, W. T., and Flannery, B. P., *Numerical Recipes in C: The Art of Scientific Computing*, 2nd ed., Cambridge Univ. Press, New York, 1997, pp. 408–412.